Pergamon

Int. J. Mech. Sci. Vol. 38, No. 5, pp. 461–482, 1996

0020-7403/96 $15.00 + 0.00

0020-7403(95)00094-1

THE SHAFT BEHAVIOR OF BTA DEEP HOLE DRILLING TOOL

JIH-HUA CHIN, CHI-TI HSIEH and LI-WEI LEE

Department of Mechanical Engineering, National Chiao Tung University, 1001 Ta Hsueh Road, Hsinchu, Taiwan, R.O.C.

(*Received* 19 *July* 1993; *and in revised form* 24 *January* 1994)

Abstract—This paper is a study on the shaft behavior of BTA deep hole drilling tool. The dynamics of tool shaft are often taken to be that of a second order lumped mass system for other cutting processes. This simplification does not apply for deep hole drilling because of its shaft length and the fact of fluid coupling. This paper constructed the general equations of motion for the pipe-like fluid conveying tool shaft of deep hole drill. The proposed general equations can be reduced to different specific forms of former works. Solutions for lateral and longitudinal motions were given. Series of experiments were designed and performed. Comparisons between theoretical and experimental results confirmed the validity of the constructed equations. The studies disclosed build the knowledge about the tool shaft and pave the way for future research concerning the correlation between the tool shaft and cutting process taking place on the cutting head.

Key words: deep hole drilling, shaft behavior, pipes, Bernoulli–Eulerian theory.

NOTATION

A_f, A_s	area of the cross section of the fluid flow, drill tube, respectively, m^2
c	viscous damping coefficient in longitudinal and lateral vibration
C_f	centroid of area A_f of the fluid flow
C_s	centroid of area A_s of the drill tube
c_T	viscous damping coefficient in torsional vibration
E	Young's modulus of the drill tube, Pa
$\vec{F}$	force resultant on the cross section of the drill tube, N
f_q	fluid quality, l/min
G	shearing modulus of the drill tube, Pa
$\vec{g}$	gravity
I_f, I_s	the moment of inertia of the area A_f, A_s, respectively, m^4
I_{xf}, I_{yf}	the moment of inertia of the area A_f with respect to x, y axis, respectively, m^4
I_{xs}, I_{ys}	the moment of inertia of the area A_s with respect to x, y axis, respectively, m^4
I_{zf}, I_{zs}	the polar moment of inertia of the area A_f, A_s, respectively, m^4
J_l	mass moment of inertia of drill head, $kg \cdot m^2$
k, k^1	components of curvature of the strained central line of the drill tube, 1/m,
l	length of drill tube, m
$\vec{M}_e$	coupled resultants about S_s on the cross section of the drill tube, N·m
$\vec{M}_G$	coupled resultants about C_s on the cross section of the drill tube, N·m
m_l	mass of drill head, kg
N	tension, N
N_l	tension at the centroid of the cross section on the tool head, N
O_f	mass center of the small element of the fluid flow
O_s	mass center of the small element of the drill tube
P	fluid pressure, N/m^2
P_l	fluid pressure on the tool head, N/m^2
$\vec{R}$	displacement of a point P_1 on the central line axis of the drill tube, m
$\vec{r}$	location of a point P on the strained central line axis of the drill tube, m
$\vec{r}_1$	location of a point P_1 on the central line axis of the drill tube, m
$\vec{r}_f$	location of fluid at the O_f, m
s	arc length of the strained central line of the drill tube, m
S_s	shear center of area A_s of the drill tube
t	time s
T_l	torque at the centroid of the cross section on the tool head, N·m
$\vec{t}_1$, $\vec{t}_2$, $\vec{t}_3$	unit vector in the direction x, y, z, respectively
U	fluid velocity, m/S
$u(s, t)$, $v(s, t)$, $w(s, t)$	component of $\vec{R}$ in the direction X, Y, Z, respectively, m

V_x, V_y shearing force in direction $\vec{t}_1$, $\vec{t}_2$, respectively, N
W eigencolumn matrix, $2M \times 2M$
$X(s,t)$, $Y(s,t)$, $Z(s,t)$ component of $\vec{r}$ in the direction X, Y, Z, respectively, m
δ unit impulse function
ε extension of the central line of the drill tube
θ angle of twist
λ eigenvalue
μ absolute viscosity, kg/m·s
ρ_f, ρ_s density of fluid, drill tube, respectively, kg/m^3
τ twist of the shaft, 1/m
$\vec{q}_s$, $\vec{q}_f$ force per unit length at the point O_s, O_f, respectively
$\vec{q}_{es}$, $\vec{q}_{ef}$ external force per unit length at the point O_s, O_s respectively
$\vec{\Lambda}_s$, $\vec{\Lambda}_f$ moment per unit length at the point O_s, O_f, respectively
$\vec{\Lambda}_{es}$, $\vec{\Lambda}_{ef}$ external moment per unit length at the point O_s, O_f, respectively

1. INTRODUCTION

A deep hole drilling machine can drill deep holes with depth-diameter-ratio above 100 due to its special design and construction. In a deep hole drilling operation, good hole tolerances with respect to bore diameter, roundness and straightness [1] can be obtained. The hole surface qualities equal those from reaming, honing and grinding, sometimes even surpassing them.

With such excellent machining performance, deep hole drillings are often applied in high precision manufacturing such as the military industry, machine tool and automobile industries. Applications examples are hydraulic cylinders, landing gears for aircraft, large holes in diesel truck applications, turbines, heat exchangers, and oil industry components, etc. [2].

There are three kinds deep hole drilling, namely, gun drilling, BTA(Boring and Trepanning Association) and ejector drilling. The gun drilling is used for a small size of hole and the BTA or ejector drilling is used for a large size of hole. In a deep hole drilling process the pressurized coolant is used.

1.1. *Purpose of the study*

Because of its length, the shaft dynamics of the deep hole drilling influences the quality of cutting process on the tool head. The deflection due to lateral bending and vibration worsens the axial hole deviation, tolerance, straightness, roundness, etc.

The purpose of this study is to establish a system model and investigate the dynamics of the shaft behavior of deep hole drilling tool theoretically and experimentally.

The behavior is correlative with the effect of fluid flow and structural dynamics. In this study we use the theories of pipes and tubes conveying fluid, with a velocity and Bernoulli–Eulerian theory containing symmetric bending and torsion to find the shaft behavior of the deep hole drilling.

1.2. *Literature review*

Flegel [1] published the quality of the deep hole drilling processes. Rudd and Hetherington [2] explain each of the three deep hole drilling processes. Rao and Shunmugam [3–6] made many experiments about hole size, axis deviation, roundness error, surface finish, axial and transverse profiles of the holes of drilled length, and wear of center, supporting pad of BTA drilling tool for many different machining conditions such as cutting speed, feed rate, cutting time, etc.. El-Khabeery, *et al.* [7] made experiments about surface integrity of deep drilling holes (such as surface roughness, hardness, micro hardness, plastic deformation of the surface and subsurface layers) for many machining conditions. For example, drilling speed, feed rate and work hole diameter in gun drilling processes. Corney and Griffiths [8] presented experiments analyzing the combined cutting and burnishing action in which the forces generated at a single cutting edge are balanced by the rubbing pad in the BTA drilling process. Sakuma *et al.* [9] made experiments and proposed simple formulas about the burnishing action of guide pads and influence on hole accuracies for machining conditions such as cutting forces, cutting torque, depth of deformation, and waves on burnished surface in the BTA process.

Sakuma *et al.* [10] found that the frequency of the bending vibration of the boring bar during machining of the holes corresponds to the number of the corners of the hole. Simple models of the support and boring bar was proposed by Sakuma *et al.* [10], but there were no complete considerations about motions, for example, the bending and torsional vibration of the shaft conveying fluid flow. Katsuti *et al.* [11] proposed comparison of single- and multi-edge tools for many conditions such as wall thickness, hardness of the bonded plate, etc.. This paper presented simple models for cutting forces.

Yumshtyk and Kedrov [12] investigated the gun drill vibration with a very simple model which considered the lateral vibration by neglecting drill length, torsional vibration and the effect of the fluid flow. Sakuma *et al.* [13] presented the deflections of misalignment in tool pilot bush or bar support on the straightness error of a drilled hole, but there were no considerations about complete motion and fluid flow. Some guide values about gun drills, BTA drills and ejector drills, for example, cutting speed, feed, net power, cutting fluid quantity, cutting fluid pressure, etc. can be found in Ref. [14].

Chin *et al.* [15] proposed the theory of signal of chip formation and proved it experimentally. Detailed mathematics concerning chip signals were given by Chin and Wu [16]. Chin and Lin [17] discussed the stability of the drilling process by treating the tool shaft as a second order lumped mass system. Chandrashekhar *et al.* [18] proposed a three-dimensional model of the BTA machining system including the interaction between the workpiece and cutting tool. A physical model for stationary workpiece and rotating cutting tool was proposed. The modes method along with Lagrange's equation was used to obtain lateral and torsional vibration equations to represent the influence of axial force and torque. Chandrashekhar *et al.* [19] found the solutions and predicted the helical grooves which were observed on the drilled workpieces, and compared theories with experiments on roundness error, but there were obvious discrepancies between theoretical and experimental results. The radial and tangential forces were not considered in Ref. [19]; the velocity of fluid was held constant in the BTA drilling processes, and the vibration solution only considered the fundamental mode.

The papers below proposed the theories of pipes and tubes containing a fluid flow. Blevins [20] proposed the planar lateral motion of the pipes with constant velocity of fluid flow, and the critical flow velocity due to the buckling of the pipe and due to the flutter. Paidoussis [21] proposed the extension of gravity on hanging cantilever tubes. Paidoussis and Issid [22] proposed the extension of the fluctuation velocity of fluid flow. Yoshizawa *et al.* [23] proposed another method about the theory of the pipes conveying fluid with fluctuation velocity, and obtained critical flow velocity and maximum values of the static deflection of the buckling pipes. Thompson and Lunn [24] presented static elastic formulation and concluded that the net effect of the fluid flow in the static case was to add an end follower thrust to the mechanically applied forces. Lundgren *et al.* [25] investigated the three-dimensional lateral vibration of the tubes of uniform annular cross section containing fluid flow with constant velocity. The papers above investigated the lateral vibrational of the pipes with double symmetric cross section, and neglected rotary inertia. Edelstein *et al.* [26] applied the finite element method to the same equation described in [25] to obtain the oscillations. Hill and Swanson [27] proposed the lumped masses on the tubes conveying fluid. Sugiyama *et al.* [28] studied the spring effect on pipes conveying fluid and proposed the criterion of stability and critical flow velocity. The pipe theory above covered the stability and critical velocity due to flutter but did not consider the axial force, critical axial force and critical fluid pressure.

Literature investigation reveals that there are no rigorous equations of motion available that govern the tool shaft of the BTA deep hold drill. In this paper the three-dimensional general equations of motion for lateral, longitudinal and torsional motion of the shaft containing the fluid flow are constructed. Specific equations solutions are given for lateral and longitudinal motions. Finally, the proposed equations for lateral motions are verified by experiments.

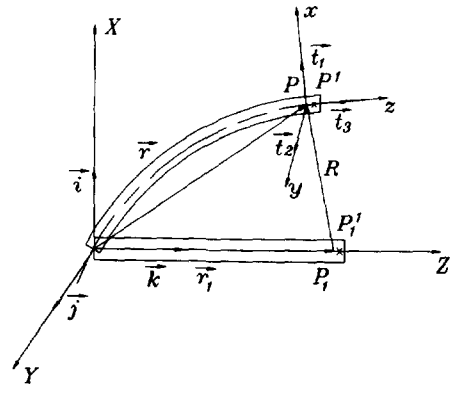

Fig. 1. Relation between the location $\vec{r}$ and the displacement $\vec{R}$.

2. EQUATIONS OF MOTION

The system under consideration consists of a shaft, conveying a fluid. The temperature and nozzle effect are neglected. The basic assumptions for the shaft are as follows:

1. Elastic homogeneous isotropic material is considered.
2. No shear deformation is considered.
3. Plane sections before deformation remain plane during deformation because of the Bernoulli–Euler theory.
4. The shaft is of uniform and thin-walled closed cross section and is initially straight.
5. Warping deformation is neglected and shaft deflection is small.

2.1. *Bernoulli–Eulerian theory*

The determination of orientation of shaft element conforms to Love [29]. Figure 1 shows the coordinates of a slightly displaced tool shaft. Let P_1^1 be a point on the central-line near P_1, and P^1 be the displaced position of P_1^1. The length of the arc $P\,P^1$ is designated by δ_s.

The location of a point P on the shaft axis is given by

$$\vec{r} = X(s, t)\vec{i} + Y(s, t)\vec{j} + Z(s, t)\vec{k} \tag{1}$$

where $\vec{i}, \vec{j}, \vec{k}$ are fixed orthogonal unit vectors. The location of a point P_1 is given by

$$\vec{r}_1 = s_1\vec{k}$$

and the displacement vector is as follows:

$$\vec{R} = \vec{r} - \vec{r}_1 = u(s, t)\vec{i} + v(s, t)\vec{j} + w(s, t)\vec{k}.$$

The unit tangent vector is

$$\vec{t}_3 = \frac{\partial \vec{r}}{\partial s} = \frac{\partial X}{\partial s}\vec{i} + \frac{\partial Y}{\partial s}\vec{j} + \frac{\partial Z}{\partial s}\vec{k}. \tag{2}$$

Let the force and torque on the cross section of the shaft be $\vec{F}$ and $\vec{M}_G$ with

$$\vec{F} = V_x\vec{t}_1 + V_y\vec{t}_2 + N\vec{t}_3 \tag{3}$$

where V_x, V_y are shearing forces, and N is the tension.

If the shearing forces $V_x\vec{t}_1 + V_y\vec{t}_2$ do not act through the shear center S_s, it can be replaced by a statically equivalent system shown in Fig. 2 [30]. We obtain

$$\vec{M}_e = \vec{M}_G + S_s\vec{C}_s \times (V_x\vec{t}_1 + V_y\vec{t}_2) \tag{4}$$

where C_s is the centroid.

Applying the Bernoulli–Eulerian theory yields

$$\vec{M}_e = \mathrm{E}I_{xs}k\vec{t}_1 + \mathrm{E}I_{ys}k^1\vec{t}_2 + C_r\tau \tag{5}$$

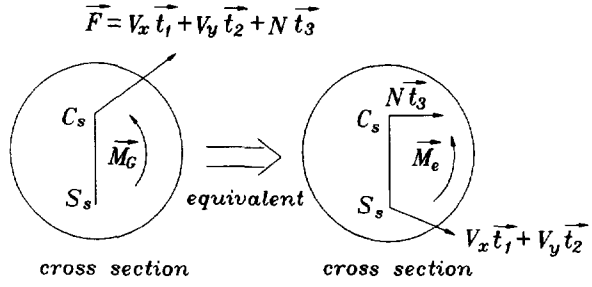

Fig. 2. Statically equivalent system.

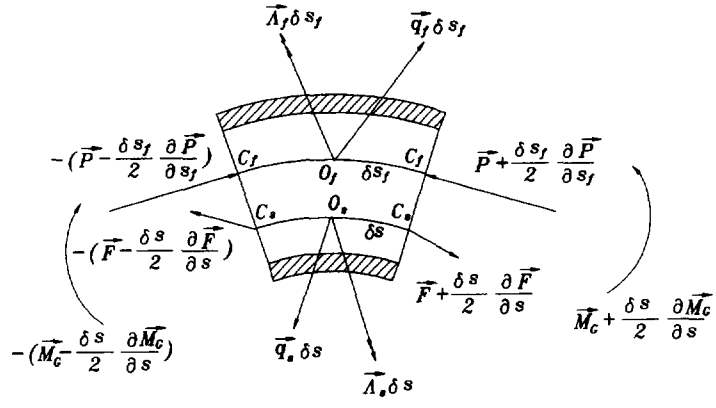

Fig. 3. The small element cut from the shaft.

where k and k^1 are the component of curvature of the strained central line, τ is the twist of the shaft and C_r is the torsional with

$$C_r = GJ.$$

2.2. *Effect of fluid flow*

Consider a small element of the shaft, with length δs_f (see Fig. 3). The corresponding mass of the enclosed fluid is δm_f. ρ_f is the density of fluid. Then

$$\delta m_f = \rho_f A_f \delta s_f.$$

The rate of change of momentum $\vec{L}_f$ can be written as:

$$\frac{d\vec{L}_f}{dt} = \rho_f A_f \delta s_f \left(\frac{\partial^2 \vec{r}_f}{\partial t^2} + 2U \frac{\partial^2 \vec{r}_f}{\partial t \partial s_f} + U^2 \frac{\partial^2 \vec{r}_f}{\partial s_f^2} + \frac{\partial U}{\partial t} \frac{\partial \vec{r}_f}{\partial s_f} \right) \tag{6}$$

$$\frac{d\vec{L}_f}{dt} = \rho_f A_f \delta s_f \left(\frac{\partial}{\partial t} + U \frac{\partial}{\partial s_f} \right)^2 \vec{r}_f(s_f, t). \tag{7}$$

The results agree with the papers by Blevins [20], Paiduossis and Issid [22], Yoshizawa, *et al.* [23], Lundgren *et al.* [25].

2.3. *Small deflection*

A small elements cut from the shaft is shown in Fig. 3.

Coordinate transformation yields:

$$\vec{M}_e = -EI_{xs} \frac{\partial^2 Y}{\partial s^2} \vec{t}_1 + EI_{ys} \frac{\partial^2 X}{\partial s^2} \vec{t}_2 + GJ \frac{\partial \theta}{\partial s} \vec{t}_3. \tag{8}$$

The following fundamental equation holds

$$\sum \vec{M} = \dot{\vec{H}}.$$

Let $(\dot{\vec{H}}_G)_s$ and $(\dot{\vec{H}}_G)_f$ be the rates of change of the angular momentum about O_s and O_f respectively. If the shaft deflection is small, the following equation can be obtained:

$$(\dot{\vec{H}}_G)_s = -I^1_{xs}\frac{\partial^3 Y}{\partial t^2 \partial s}\vec{t}_1 + I^1_{ys}\frac{\partial^3 X}{\partial t^2 \partial s}\vec{t}_2 + I^1_{zs}\frac{\partial^3 \theta}{\partial t^2}\vec{t}_3$$

where I^1_{xs}, I^1_{ys}, I^1_{zs} denote the principal centroidal moments of inertia and

$$I^1_{xs} = \rho_s I_{xs}\delta s; \quad I^1_{ys} = \rho_s I_{ys}\delta s; \quad I^1_{zs} = \rho_s I_{zs}\delta s.$$

Let

$$(\dot{\vec{H}}_G)_s = \rho_s \vec{h}_{gs}\delta s$$

then

$$\vec{h}_{gs} = -I_{xs}\frac{\partial^3 Y}{\partial t^2 \partial s}\vec{t}_1 + I_{ys}\frac{\partial^3 X}{\partial t^2 \partial s}\vec{t}_2 + I_{zs}\frac{\partial^2 \theta}{\partial t^2}\vec{t}_3. \tag{9}$$

Similarly,

$$\vec{h}_{gf} = -I_{xf}\frac{\partial^3 Y}{\partial t^2 \partial s_f}\vec{t}_1 + I_{yf}\frac{\partial^3 X}{\partial t^2 \partial s_f}\vec{t}_2 + I_{zf}\frac{\partial^2 \theta}{\partial t^2}\vec{t}_3 \tag{10}$$

and the tension is:

$$N = \mathrm{E}A_s\frac{\partial w}{\partial s}. \tag{11}$$

2.4. *Equations of motion of BTA drill shaft with stationary cutting tool*

In BTA drilling processes, the shaft is of uniform annular cross section, the points C_s, C_f, S_s are of the same location, and the points O_s, O_f become identical. So we can take:

$$I_{xs} = I_{ys} = I_s; \quad I_{xf} = I_{yf} = I_f$$

$$s_f = s; \quad \vec{r}_f = \vec{r}$$

and the flow velocity U is opposite to the direction defined earlier, so the rate of change of momentum $\vec{L}_f$ of BTA drill becomes:

$$\frac{\mathrm{d}\vec{L}_f}{\mathrm{d}t} = \rho_f A_f \delta s\left(\frac{\partial}{\partial t} - U\frac{\partial}{\partial s}\right)^2 \vec{r}(s, t).$$

The force equation is:

$$\frac{\partial \vec{F}}{\partial s} + \frac{\partial \vec{P}}{\partial s} + \vec{q}_s + \vec{q}_f = 0 \tag{12}$$

where

$$\vec{q}_s = -\rho_s A_s\frac{\partial^2 \vec{r}}{\partial t^2} + \rho_s A_s \vec{g} + \vec{q}_{es}$$

$$\vec{q}_f = -\rho_f A_f\left(\frac{\partial}{\partial t} + U\frac{\partial}{\partial s_f}\right)^2 \vec{r}_f + \rho_f A_f \vec{g} + \vec{q}_{ef}.$$

The moment equation is:

$$\vec{t}_3 \times \vec{F} + \vec{t}_3 \times \vec{P} + \frac{\partial \vec{M}_G}{\partial s} + \vec{\Lambda}_s + \vec{\Lambda}_f = 0 \tag{13}$$

where

$$\vec{\Lambda}_s = -\rho_s \vec{h}_{gs} + \vec{\Lambda}_{es}$$

$$\vec{\Lambda}_f = -\rho_f \vec{h}_{gf} + \vec{\Lambda}_{ef}.$$

The following relations can be established from Fig. 4:

$$\vec{F} = N\vec{t}_3 + \vec{t}_3 \times \left(\frac{\partial \vec{M}_G}{\partial s} + \vec{\Lambda}_s + \vec{\Lambda}_f\right). \tag{14}$$

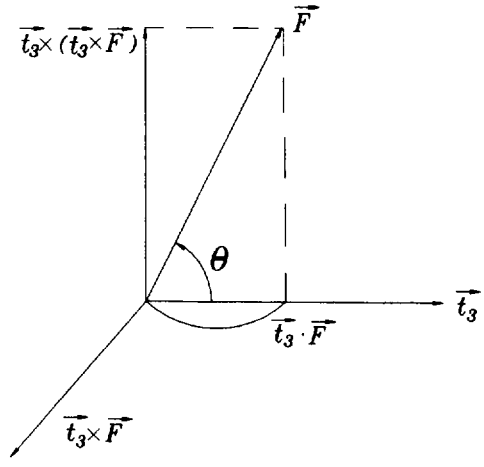

Fig. 4. The relationship of the force in rectangular coordinates.

Substituting Eqn (14) into Eqn (12), the following general force equation can be obtained

$$-\frac{\partial^2}{\partial s^2}\left(EI_s\frac{\partial^2\vec{r}}{\partial s^2}\right)-\frac{\partial}{\partial s}\left(EI_s k_n^2\frac{\partial\vec{r}}{\partial s}\right)+\frac{\partial}{\partial s}\left(GJ\tau\frac{\partial\vec{r}}{\partial s}\times\frac{\partial^2\vec{r}}{\partial s^2}\right)$$
$$\frac{\partial}{\partial s}\left[(\rho_s I_s+\rho_f I_f)\frac{\partial^3 X}{\partial t^2\partial s}\right]\vec{t}_1+\frac{\partial}{\partial s}\left[(\rho_s I_s+\rho_f I_f)\frac{\partial^3 Y}{\partial t^2\partial s}\right]\vec{t}_2$$
$$+\frac{\partial}{\partial s}\left[(N-PA_f)\frac{\partial\vec{r}}{\partial s}\right]-\rho_s A_s\frac{\partial^2\vec{r}}{\partial t^2}-\rho_f A_f\left(\frac{\partial}{\partial t}+U\frac{\partial}{\partial s}\right)^2\vec{r}$$
$$+(\rho_s A_s+\rho_f A_f)\vec{g}+\vec{q}_{es}+\vec{q}_{ef}+\frac{\partial}{\partial s}[\vec{t}_3\times(\vec{\Lambda}_{es}+\vec{\Lambda}_{ef})]=0. \tag{15}$$

If we do not consider the twist τ, the gravity $\vec{g}$, the external force, the external moment, the rate of the change of the momentum $\frac{\partial}{\partial s}(\rho_s I_s\frac{\partial^3 X}{\partial t^2\partial s})\ldots$, it is the same as the equation in Refs [25] and [26]. If we also neglect the k_n, it is the same as the equation in Ref. [20].

From $\vec{i}\cdot$ in Eqn (15) the following form can be obtained by neglecting the high order terms

$$-\frac{\partial^2}{\partial s^2}\left(EI_s\frac{\partial^2 X}{\partial s^2}\right)+\frac{\partial}{\partial s}\left[(\rho_s I_s+\rho_f I_f)\frac{\partial^3 X}{\partial t^2\partial s}\right]+\frac{\partial}{\partial s}\left[(N-PA_f)\frac{\partial X}{\partial s}\right]$$
$$-\rho_s A_s\frac{\partial^2 X}{\partial t^2}-\rho_f A_f\left(\frac{\partial}{\partial t}+U\frac{\partial}{\partial s}\right)^2 X-(\rho_s A_s+\rho_f A_f)g$$
$$+\vec{i}\cdot(\vec{q}_{es}+\vec{q}_{ef})+\vec{i}\cdot\frac{\partial}{\partial s}[\vec{t}_3\times(\vec{\Lambda}_{es}+\vec{\Lambda}_{ef})]=0. \tag{16}$$

If we do not consider the twist τ, the gravity $\vec{g}$, the external force, the external moment, the pressure P of the fluid flow, it is the same as the equation in Refs [18] and [19].

From $\vec{t}_3\cdot$ in Eqn (15) the following equation is obtained

$$2\frac{\partial}{\partial s}(EI_s)k_n^2+EI_s\frac{\partial}{\partial s}\left(\frac{1}{2}k_n^2\right)+\vec{t}_3\cdot\frac{\partial}{\partial s}\left(GJ\tau\frac{\partial\vec{r}}{\partial s}\times\frac{\partial^2\vec{r}}{\partial s^2}\right)$$
$$+\frac{\partial}{\partial s}(N-PA_f)-\rho_f A_f\frac{\partial U}{\partial t}-(\rho_s A_s+\rho_f A_f)\vec{t}_3\cdot\frac{\partial^2\vec{r}}{\partial t^2}$$
$$+(\rho_s A_s+\rho_f A_f)\vec{t}_3\cdot\vec{g}+\vec{t}_3\cdot(\vec{q}_{es}+\vec{q}_{ef})$$
$$+\vec{t}_3\cdot\frac{\partial}{\partial s}[\vec{t}_3\times(\vec{\Lambda}_{es}+\vec{\Lambda}_{ef})]=0 \tag{17}$$

where k_n is curvature in the normal direction $k_n=|\frac{\partial\vec{t}_3}{\partial s}|=|\frac{\partial^2\vec{r}}{\partial s^2}|$.

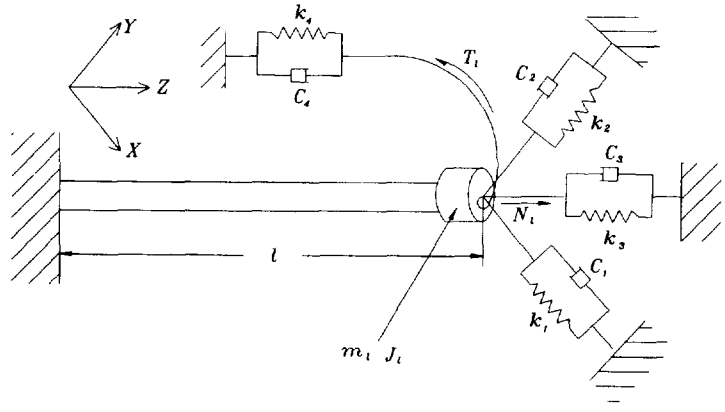

Fig. 5. Boundary condition on the tool head.

If E, I_s, U are constant and the twist τ, gravity $\vec{g}$, external force, external moment are neglected, it is the same as the equation in Refs [25] and [26].

2.5. *Boundary conditions*

The boundary conditions are constructed as that shown in Fig. 5. The condition at location $s = l$ can be expressed by two models.

Model 1. The boundary condition contains the mass m_l, the moment of inertia of mass J_l, the forces, the torque, the springs and the dampers.

Model 2. The boundary condition at $s = l$ is free while the mass m_l, the moment of inertia of mass J_l, the forces, the torque, the springs and the dampers are replaced by concentrated forces and torques.

3. THE SOLUTIONS OF EQUATIONS OF MOTION

The solutions of equations of motion of the BTA drill shaft will be given for the following general cases:

$$\vec{q}_{es} = -c\frac{\partial \vec{r}}{\partial t} + f_1(s,t)\vec{i} + f_2(s,t)\vec{j} + f_3(s,t)\vec{k} \tag{18}$$

where $-c\frac{\partial \vec{r}}{\partial t}$ denotes viscous damping force and f_1, f_2, f_3, are the external forces per unit length.

$$\vec{q}_{ef} = 0 \tag{19}$$

$$\vec{\Lambda}_{es} = -c_t\frac{\partial \theta}{\partial t}\vec{i}_2 + f_4(s,t)\vec{k} \tag{20}$$

where $-c_t\frac{\partial \theta}{\partial t}$ denotes viscous damping torque and f_4 is the external torque per unit length.

$$\vec{\Lambda}_{ef} = 0. \tag{21}$$

3.1. *Lateral motion of the shaft*

The equation of motion for lateral motion can be derived from Eqn (16):

$$-\mathrm{E}I_s\frac{\partial^4 X}{\partial s^4} + (\rho_s I_s + \rho_f I_f)\frac{\partial^4 X}{\partial t^2 \partial s^2} + \frac{\partial}{\partial s}\left[(N - PA_f)\frac{\partial X}{\partial s}\right]$$
$$-\rho_s A_s\frac{\partial^2 X}{\partial t^2} - \rho_f A_f\left(\frac{\partial}{\partial t} + U\frac{\partial}{\partial s}\right)X - (\rho_s A_s + \rho_f A_f)g$$
$$-c\frac{\partial X}{\partial t} + f_1(s,t) = 0. \tag{22}$$

B.C.'s

$$s = 0, \quad X = 0, \quad \frac{\partial X}{\partial s} = 0$$

$$s = l, \quad \mathrm{E}I_s \frac{\partial^2 X}{\partial s^2} = 0$$

$$s = l, \quad \mathrm{E}I_s \frac{\partial^3 X}{\partial s^3} = -m_l \frac{\partial^2 X}{\partial t^2} - c_1 \frac{\partial X}{\partial t} - k_1 X - N_l \frac{\partial X}{\partial s}.$$

If m_l, c_1 in boundary condition are neglected it is similar to the equation in Ref. [22]. I.C.s

$$t = 0, \quad X = g_{x1}(s)$$

$$t = 0, \quad \frac{\mathrm{d}X}{\mathrm{d}t} = g_{x2}(s).$$

Assume the solution of Eqn (22) is of following form:

$$X(s, t) = X_1(s, t) + X_2(s).$$

We first find $X_2(s)$ by applying model 1 of the boundary conditions.
Suppose

$$X_2 = X_{2h} + X_{2p}$$

where X_{2h} is the homogeneous solution and X_{2p} is the particular solution. We have

$$X_{2p} = -\frac{s^2(\rho_s A_s + \rho_f A_f)g}{2(-N_1 + P_l A_f + \rho_f A_f U^2)}.$$

Because $N_l < 0$ which is a compressive force we have

$$b_v^2 = \frac{-N_l + P_l A_f + \rho_f A_f U^2}{\mathrm{E}I_s}$$

$$X_{2h} = d_1 \sin b_v s + d_2 \cos b_v s - d_1 b_v s - d_2$$

where d_1, d_2 can be obtained from the following two linear equations:

$$\frac{\partial^2 X_2(l)}{\partial s^2} = -d_1 b_v^2 \sin b_v l - d_2 b_v^2 \cos b_v l - \frac{(\rho_s A_s + \rho_f A_f)g}{-N_l + P_l A_f + \rho_l A_f U^2} = 0$$

$$-\mathrm{E}I_s(-d_1 b_v^3 \cos b_v l + d_2 b_v^3 \sin b_v l) =$$

$$-k_1\left[d_1(\sin b_v l - b_v l) + d_2(\cos b_v l - 1)\right.$$

$$\left.-\frac{l^2(\rho_s A_s + \rho_f A_f)g}{2(-N_l + P_l A_f + \rho_f A_f U^2)}\right] - N_l\left[d_1(b_v \cos b_v l) - d_2 b_v \sin b_v l\right.$$

$$\left.-\frac{l(\rho_s A_s + \rho_f A_f)g}{-N_l + P_l A_f + \rho_f A_f U^2}\right].$$

It is convenient to introduce the dimensionless quantities for X_1:

$$\bar{X}_1 = \frac{X_1}{l}, \quad \bar{s} = \frac{s}{l}$$

$$\bar{t} = t\frac{1}{l^2}\left(\frac{\mathrm{E}I_s}{\rho_s A_s + \rho_f A_f}\right)^{1/2}$$

$$\bar{I}_p = \frac{\rho_s I_s + \rho_f I_f}{l^2(\rho_s A_s + \rho_f A_f)}, \quad U = Ul\left(\frac{\rho_f A_f}{\mathrm{E}I_s}\right)^{1/2}$$

$$\bar{\rho}_f = \frac{\rho_f A_f}{\rho_s A_s + \rho_f A_f}, \quad \bar{c} = c \frac{l^2}{[EI_s(\rho_s A_s + \rho_f A_f)]^{1/2}}$$

$$\bar{m}_l = \frac{m_l}{l(\rho_s A_s + \rho_f A_f)}, \quad \bar{c}_1 = c_1 \frac{l}{[EI_s(\rho_s A_s + \rho_f A_f)]^{1/2}}$$

$$\bar{k}_1 = k_1 \frac{l^3}{EI_s}, \quad \bar{N}_l = N_l \frac{l^2}{EI_s}, \quad \bar{P}_l = P_l A_f \frac{l^2}{EI_s}$$

$$\bar{f}_1 = f_1 \frac{l^3}{EI_s}, \quad \bar{g}_{x3} = \frac{g_{x3}}{l}$$

$$\bar{q}_{x4} = g_{x4} l \left(\frac{\rho_s A_s + \rho_f A_f}{EI_s}\right)^{1/2}, \quad \omega = \Omega l^2 \left(\frac{\rho_s A_s + \rho_f A_f}{EI_s}\right)^{1/2}$$

and the equation is rearranged as:

$$\frac{\partial^4 \bar{X}_1}{\partial \bar{s}^4} - \bar{I}_\rho \frac{\partial^4 \bar{X}_1}{\partial \bar{t}^2 \partial \bar{s}^2} + N_l \delta(\bar{s} - 1) \frac{\partial \bar{X}_1}{\partial \bar{s}}$$

$$- (\bar{N}_l - \bar{P}_l) \frac{\partial^2 \bar{X}_1}{\partial \bar{s}^2} + \frac{\partial^2 \bar{X}_1}{\partial \bar{t}^2} + 2\bar{U} \bar{\rho}_f^{1/2} \frac{\partial^2 \bar{X}_1}{\partial \bar{t} \partial \bar{s}}$$

$$+ \bar{U}^2 \frac{\partial^2 \bar{X}_1}{\partial \bar{s}^2} + \bar{c} \frac{\partial \bar{X}_1}{\partial t} + \bar{m}_l \delta(\bar{s} - 1) \frac{\partial^2 \bar{X}_1}{\partial \bar{t}^2}$$

$$+ \bar{c}_1 \delta(\bar{s} - 1) \frac{\partial \bar{X}_1}{\partial \bar{t}} + \bar{k}_1 \delta(\bar{s} - 1) \bar{X}_1 = \bar{f}_1(\bar{s}, \bar{t}) \tag{23}$$

with B.C.'s

$$\bar{s} = 0, \quad \bar{X}_1 = 0, \quad \frac{\partial \bar{X}_1}{\partial \bar{s}} = 0$$

$$\bar{s} = 1, \quad \frac{\partial^2 \bar{X}_1}{\partial \bar{s}^2} = 0, \quad \frac{\partial^3 \bar{X}_1}{\partial \bar{s}^3} = 0.$$

The *Galerkin method* is used to find X_1. Suppose that

$$\bar{X}_1(\bar{s}, \bar{t}) = \sum_{m=1}^{M} \phi_m(\bar{s}) q_m(\bar{t}) \tag{24}$$

where $\phi_m(\bar{s})$ satisfy all the boundary conditions of the system.

We take

$$\phi_m(\bar{s}) = \cosh \beta_m \bar{s} - \cos \beta_m \bar{s} - \sigma_m(\sinh \beta_m \bar{s} - \sin \beta_m \bar{s}) \tag{25}$$

where β_m satisfies the equation

$$\cos \beta_m \cosh \beta_m + 1 = 0 \tag{26}$$

and

$$\sigma_m = \frac{\sinh \beta_m - \sin \beta_m}{\cosh \beta_m + \cos \beta_m}.$$

By the Galerkin method, the following equation in matrix form can be obtained:

$$A\ddot{q} + B\dot{q} + Cq = f(\bar{t}) \tag{27}$$

where A, B, C are $M \times M$ matrices and q, f, Φ are $M \times 1$ matrices. We can write:

$$X_1(\bar{s}, \bar{t}) = \Phi^T(\bar{s}) q(\bar{t}) \tag{28}$$

where $q(\bar{t})$ is of the following form [31]:

$$q(\bar{t}) = W_{up}\, e^{\bar{t}J} \int_0^{\bar{t}} e^{-\tau J}\, W_{ri}^{-1}\, A^{-1} f(\tau)\mathrm{d}\tau + W_{up}\, e^{\bar{t}J}\, W^{-1} \begin{Bmatrix} q(0) \\ \dot{q}(0) \end{Bmatrix} \tag{29}$$

where J is the Jordan matrix, $W = [W_{up}\ W_{lo}]^{\mathrm{T}}$, $W^{-1} = [W_{le}^{-1}\ W_{ri}^{-1}]$, W = eigencolumn matrix.

The matrices $q(0)$, $\dot{q}(0)$ are found by using I.C. and the orthogonality of $\phi_m(\bar{s})$ as follows:

$$q_m(0) = \int_0^1 \phi_m(\bar{s})\bar{g}_{x3}(\bar{s})\mathrm{d}\bar{s}$$

$$\dot{q}_m(0) = \int_0^1 \phi_m(\bar{s})\bar{g}_{x4}(\bar{s})\mathrm{d}\bar{s}.$$

Finally, we obtain

$$X_1(s, t) = X_1(\bar{s}, \bar{t})l = l\Phi^{\mathrm{T}}(\bar{s})q(\bar{t})$$

$$X(s, t) = X_1(s, t) + X_2(s).$$

This completes the solution of equations for lateral shaft motion. $Y(s, t)$ can be obtained in a similar way by neglecting gravity.

3.2. *Longitudinal motion of the shaft*

The equation of motion for longitudinal motion can be derived from Eqn (17):

$$EA_s \frac{\partial^2 w}{\partial s^2} - P_d A_f - (\rho_s A_s + \rho_f A_f)\frac{\partial^2 w}{\partial t^2} - c\frac{\partial w}{\partial t} + f_3(s, t) = 0 \tag{30}$$

where $P_d = \frac{\partial p}{\partial s} = -\frac{8\mu U}{R^2}$ [32].

B.C.'s:

$$s = 0, \quad w = 0$$

$$s = l, \quad EA_s \frac{\partial w}{\partial s} = -m_l \frac{\partial^2 w}{\partial t^2} - k_3 w - c_3 \frac{\partial w}{\partial t} + N_l$$

I.C.'s

$$t = 0, \quad w(s, 0) = g_1(s)$$

$$t = 0, \quad \dot{w}(s, 0) = g_2(s).$$

Assume the solution of Eqn (30) is of following form:

$$w(s, t) = w_1(s, t) + w_2(s).$$

We first find the static solution $w_2(s)$ by solving the following reduced equation:

$$EA_s \frac{\partial^2 w_2}{\partial s^2} - P_d A_f = 0.$$

It leads to

$$w_2(s) = \frac{P_d A_f}{EA_s}\left(\frac{1}{2}s^2 - Ls + \frac{k_3 l^2}{2(EA_s + k_3 l)}s\right) + \frac{N_l}{EA_s + k_3 l}s. \tag{31}$$

$w_1(s, t)$ is governed by the following reduced equation:

$$EA_s \frac{\partial^2 w_1}{\partial s^2} - (\rho_s A_s + \rho_f A_f)\frac{\partial^2 w_1}{\partial t^2} - c\frac{\partial w_1}{\partial t} + f_3(s, t) = 0$$

B.C.'s

$$s = 0, \quad w_1 = 0$$

$$s = l, \quad EA_s \frac{\partial w_1}{\partial s} = -m_l \frac{\partial^2 w_1}{\partial t^2} - c_3 \frac{\partial w_1}{\partial t} - k_3 w_1.$$

I.C.'s

$$t = 0, \quad w_1(s, 0) = g_3(s) = g_1(s) - w_2(s)$$

$$t = 0, \quad \dot{w}_1(s, 0) = g_4(s) = g_2(s).$$

It is convenient to introduce the following dimensionless quantities

$$b = \sqrt{\frac{E}{\rho_s}} \frac{1}{1 + \dfrac{\rho_f A_f}{\rho_s A_s}}$$

$$\bar{t} = t\frac{b}{l} = \frac{t}{l}\left(\frac{EA_s}{\rho_s A_s + \rho_f A_f}\right)^{1/2}$$

$$\bar{c} = c \frac{l}{[EA_s(\rho_s A_s + \rho_f A_f)]^{1/2}}$$

$$\bar{c}_3 = c_3 \frac{1}{[EA_s(\rho_s A_s + \rho_f A_f)]^{1/2}}$$

$$\bar{f}_3 = f_3 \frac{l}{EA_s}, \quad \bar{g}_3 = \frac{g_3}{l}, \quad g_4 = \frac{g_4}{b}$$

$$\omega = \Omega l \left(\frac{\rho_s A_s + \rho_f A_f}{EA_s}\right)^{1/2}$$

and the equation is normalized as

$$-\frac{\partial^2 \bar{w}_1}{\partial \bar{s}^2} + \frac{\partial^2 \bar{w}_1}{\partial \bar{t}^2} + \bar{c}\frac{\partial^2 \bar{w}_1}{\partial \bar{t}} + \bar{m}_l \frac{\partial^2 \bar{w}_1}{\partial \bar{t}^2}\delta(\bar{s} - 1)$$

$$+ \bar{c}_3 \frac{\partial \bar{w}_1}{\partial \bar{t}}\delta(\bar{s} - 1) + \bar{k}_3 \bar{w}_1 \delta(\bar{s} - 1) = \bar{f}_3(\bar{s}, \bar{t}) \tag{32}$$

with B.C.s

$$\bar{s} = 0, \quad \bar{w}_1 = 0$$

$$\bar{s} = 1, \quad \frac{\partial \bar{w}_1}{\partial \bar{s}} = 0.$$

Again the *Galerkin method* is used to find w_1. Suppose that

$$\bar{w}_1(\bar{s}, \bar{t}) = \sum_{m=1}^{M} \phi_m(\bar{s}) q_m(\bar{t}) \tag{33}$$

where $\phi_m(\bar{s})$ satisfy all the boundary condition of the system.

We take

$$\phi_m(\bar{s}) = \sin \bar{\lambda}_m \bar{s}, \quad \text{where } \bar{\lambda}_m = \frac{(2m - 1)\pi}{2}, \quad m = 1, 2, \ldots$$

The $\phi_m(\bar{s})$ are orthogonal over the span of the cantilever.

By following operation similar to that in Section 3.1, we can obtain

$$A\ddot{q} + B\dot{q} + Cq = f(\bar{t}) \tag{34}$$

where A, B, C are $M \times M$ matrices and q, f, Φ are $m \times 1$ matrices.

Using

$$q_i(0) = \frac{1}{m_{ii}}\left[\int_0^1 \phi_i(\bar{s}) g_3(\bar{s}) \mathrm{d}\bar{s}\right]$$

$$\frac{\mathrm{d}q_i(0)}{\mathrm{d}t} = \frac{1}{m_{ii}}\left[\int_0^1 \phi_i(\bar{s}) g_4(\bar{s}) \mathrm{d}\bar{s}\right]$$

Table 1. The natural frequencies of lateral vibration of the shaft of BTA drill (hanged horizontally with no fluid)

Mode	Theoretical values of Eqn (35) (Hz)	Theoretical values of Euler beam (Hz)	Experimental values (Hz)
1	36.522	36.538	38.752
2	100.629	100.718	103.469
3	197.170	197.447	199.699
4	325.541	326.390	326.396
5	485.673	487.571	492.157
6	677.275	680.987	693.670
7	900.084	906.640	914.559
8	1153.745	1164.528	1178.076

where $m_{ii} = \frac{1}{2}$, the $q(\bar{t})$ can be found by the same method is Section 3.1. Finally, we obtain

$$w_1(s, t) = \bar{w}_1(\bar{s}, \bar{t})l = l\Phi(\bar{s})q(\bar{t})$$

$$w(s, t) = \bar{w}_1(s, t) + w_2(s).$$

This completes the solution of equations for longitudinal shaft motion.

4. SYSTEM SIMPLIFICATION

The foregoing equations of motion were established in a general sense. They could be simplified to cope with the practical engineering features.

For example, the tool shaft is of steel material so that the deformation is small and the effect of rotatory inertia could be neglected. This leads to an Euler Beam. In order to make system simplification the following two preliminary system analyses are performed.

4.1. *System eigenproperties—solid shaft*

The equation of motion in lateral direction can be derived from Eqn (22) as follows:

$$EI_s \frac{\partial^4 X}{\partial s^4} + \rho_s A_s \frac{\partial^2 X}{\partial t^2} + C \frac{\partial X}{\partial t} - \rho_s I_s \frac{\partial^4 X}{\partial s^2 \partial t^2} = 0. \tag{35}$$

This equation can be further simplified to become an Euler beam equation:

$$EI_s \frac{\partial^4 X}{\partial s^4} + \rho_s A_s \frac{\partial^2 X}{\partial t^2} + C \frac{\partial X}{\partial t} = 0. \tag{36}$$

The following boundary conditions are used to investigate the shaft eigenproperties.

$$s = 0, \quad \frac{\partial^2 X}{\partial s^2} = \frac{\partial^3 X}{\partial s^3} = 0$$

$$s = l, \quad \frac{\partial^2 X}{\partial s^2} = \frac{\partial^3 X}{\partial s^3} = 0.$$

The natural frequencies of modes 1–8 of the two theories and of experiment are listed in Table 1 which reveals that theoretical values of Euler Beam are closer to the experimental values than those predicted by Eqn (35).

4.2. *System eigenproperties—solid shaft with static fluid*

The purpose of this analysis is to examine the system under the influence of the static fluid.

The equation of motion can be rewritten from Eqn (22) for lateral shaft motion as follows:

$$EI_s \frac{\partial^4 X}{\partial s^4} + (\rho_s A_s + \rho_f A_f) \frac{\partial^2 X}{\partial t^2} + C \frac{\partial X}{\partial t} - (\rho_s I_s + \rho_f I_f) \frac{\partial^4 X}{\partial s^2 \partial t^2} = 0. \tag{37}$$

Table 2. The natural frequencies of lateral vibration of the shaft of BTA drill (hanged horizontally with static fluid)

Mode	Theoretical values of Eqn (37) (Hz)	Theoretical values of Euler beam (Hz)	Experimental values (Hz)
1	34.935	34.989	34.877
2	96.258	96.338	96.881
3	188.612	188.861	189.887
4	311.432	312.195	313.895
5	464.658	466.368	472.781
6	648.028	651.373	654.917
7	861.305	867.213	868.056
8	1104.167	1113.887	1116.072

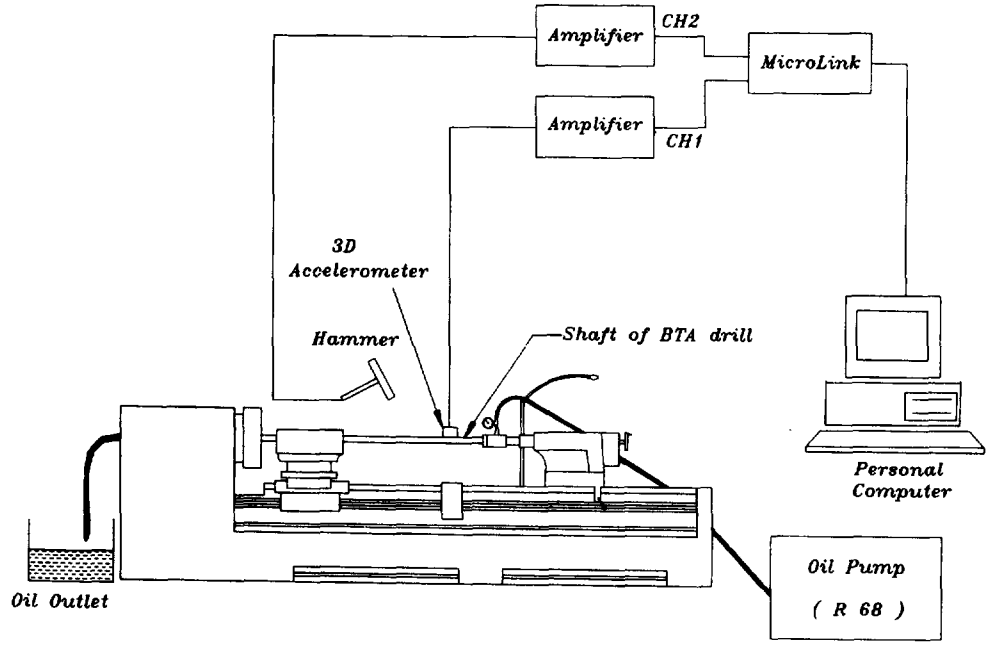

Fig. 6. The setup of experimental equipments.

The equation of motion of an Euler Beam is:

$$EI_s \frac{\partial^4 X}{\partial s^4} + (\rho_s A_s + \rho_f A_f) \frac{\partial^2 X}{\partial t^2} + C \frac{\partial X}{\partial t} = 0. \tag{38}$$

Both system equations are subjected to the same boundary conditions as that in Section 4.1.

Comparing the theoretical values of natural frequencies of modes 1–8 with those of experiment in Table 2, it is seen again that the theoretical values of an Euler Beam are closer to the experimental values than those predicted by Eqn (37).

Based on the results of the above two series of preliminary analyses, the proposed equations of motion can be simplified and the shaft of the BTA drill be taken as an Euler Beam. In the following studies only the simplified equations of motion will be used.

5. THE EXPERIMENTAL ARRANGEMENTS

The experimental arrangements are shown in Fig. 6, in which a heavy duty lathe is equipped with self-designed fixtures to hold the drill on both ends. The experiments which involve generally modal testing techniques [33, 34] are divided into two parts:

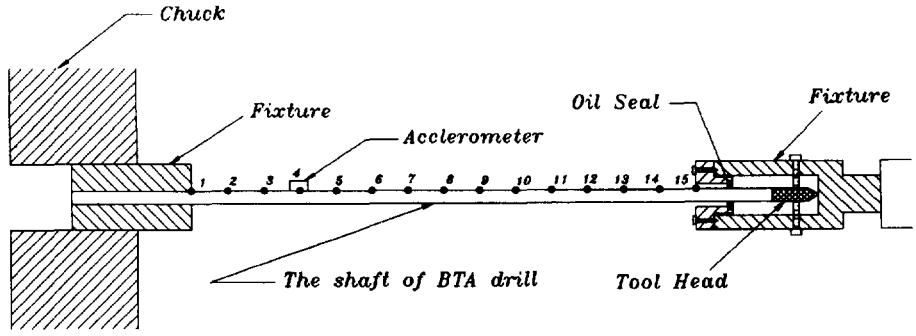

Fig. 7. The arrangements of experiment (shaft without fluid, both ends are clamped).

(1) The shaft of the BTA drill is installed on the machine without introduction of oil.
(2) The shaft of the BTA drill is installed on the machine with both ends fixed and oil is supplied.

Details of the experimental arrangements are as follows:

1. Lathe:
SAN SHING SK26120 HEAVY DUTY PRECISION LATHE.
(Distance between chuck center and tailstock center: 3m)
2. Hammer:
Hammer: PCB 086B05 SN5163 (range: 0–5000 lb)
Amplifier: PCB model 480D06 power unit.
3. Accelerometer:
accelerometer: TEAC 601Z (weight: 0.3 g)
amplifier: TEAC SA620.
4. Data acquisition system:
MicroLink: four independent channels, stand-alone type with 64k samples per channel on-board memories.
5. The deep hole drill:
a. drill head:
Type: SANDVIK 420.6-0014D 18.91 70
Mass: 0.030205 kg
Mass moment of inertia J_l: 1.420×10^{-6} kg·m^2.
b. drill tube:
Type: SANDVIK 420.5-800-2
Length: 1.6 m
Internal diameter: 11.5 mm
External diameter: 17.0 mm
Material: JIS SNCM 21
Density ρ_s: 7860 kg/m^3
Young's modulus E: 2.06×10^{11} Pa
Shear modulus G: 8.1×10^{10} Pa
6. Fluid:
Type: R68
Density ρ_f: 866 kg/m^3
Absolute viscosity μ: 0.383 kg/m·s.

6. THE SHAFT BEHAVIOR IN INSTALLED CIRCUMSTANCES

The shaft is installed on the lathe by the fixtures and the shaft behavior in installed circumstances is investigated in this section. The arrangements of this experiment are shown in Fig. 7.

The equation of lateral motion is:

$$EI_s \frac{\partial^4 X}{\partial s^4} + \rho_s A_s \frac{\partial^2 X}{\partial t^2} + C \frac{\partial X}{\partial t} = 0 \tag{39}$$

with B.C.'s

$$s = 0, \quad X = \frac{\partial X}{\partial s} = 0$$

$$s = l, \quad \frac{\partial^2 X}{\partial s^2} = \frac{\partial^3 X}{\partial s^3} = 0.$$

Table 3. The natural frequencies of lateral vibration of the shaft of BTA drill (both ends clamped horizontally with no fluid)

Mode	Theoretical values (Hz)	Experimental values (Hz)
1	44.488	44.178
2	122.634	115.958
3	240.411	230.559
4	397.412	368.149

Let

$$X(s, t) = \Sigma\phi(s)\, q(t).$$

The mode shape function $\phi_j(s)$ can be obtained from the boundary conditions:

$$\phi_j(s) - \cosh \beta_j s - \cos \beta_j s - \alpha_j(\sinh \beta_j s - \sin \beta_j s) \tag{40}$$

and

$$\alpha_j = \frac{\cosh \beta_j l - \cos \beta_j l}{\sinh \beta_j l - \sin \beta_j l}$$

$$\cosh \beta_j l \cdot \cos \beta_j l = 0.$$

Giving an impulse to the shaft yields

$$\mathrm{E}I_s \frac{\partial^4 X}{\partial s^4} + \rho_s A_s \frac{\partial^2 X}{\partial t^2} + C \frac{\partial X}{\partial t} = h(t).$$

By doing the Fourier Transform of the above equation and solving for the closed form, the solution yields

$$H_j(w) = \frac{1}{\left(1 - \dfrac{w^2}{\dfrac{\beta_j^4 \mathrm{E}I_s}{\rho_s A_s}}\right) - i\left(\dfrac{w}{\dfrac{\beta_j^4 \mathrm{E}I_s}{c_j}}\right)}. \tag{41}$$

The theoretical natural frequency is equal to

$$f_n = \frac{1}{2\pi} \sqrt{\frac{\beta_j^4\ \mathrm{E}I_s}{\rho_s A_s}}. \tag{42}$$

The frequency response function is

$$H(s_s, s_r, w) = \sum_{j=1}^{M} \phi_j(s_s)\, \phi_j(s_r)\, H_j(w).$$

a. Natural frequency

In this experiment, the tool head is fixed with two bolts and an oil seal ring is present which makes the practical boundary condition complex and not ideal. The comparisons between the theoretical and the experimental values of natural frequencies of modes 1–4 are listed in Table 3 in which the agreement can be seen, but the discrepancies are somewhat larger than that in Tables 1 and 2.

b. Mode shape

The mode shape function of the shaft is

$$\phi_j(s) = \cosh \beta_j s - \cos \beta_j s - \frac{\cosh \beta_j l - \cos \beta_j l}{\sinh \beta_j l - \sin \beta_j l} (\sinh \beta_j s - \sin \beta_j s).$$

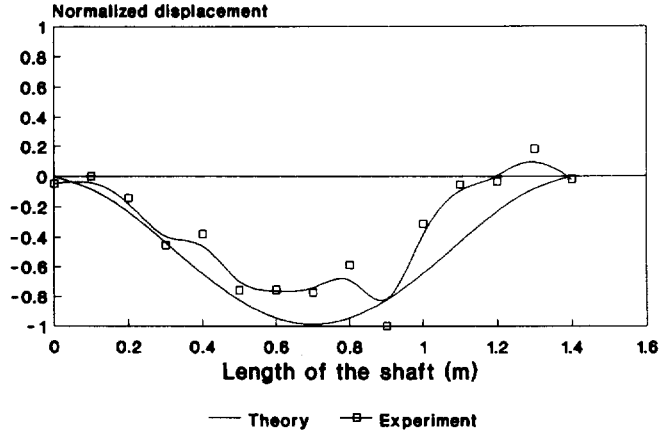

Fig. 8. The shape of mode 1 for lateral vibration (shaft without fluid, fixed–fixed).

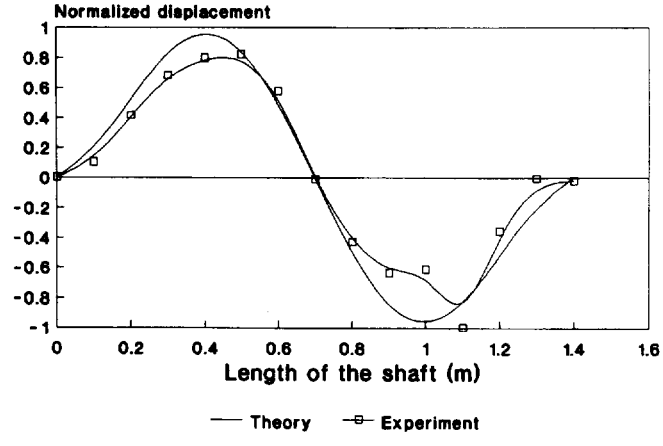

Fig. 9. The shape of mode 2 for lateral vibration (shaft without fluid, fixed–fixed).

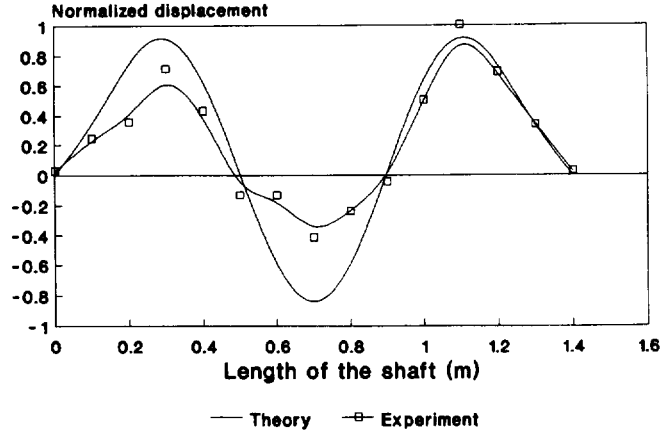

Fig. 10. The shape of mode 3 for lateral vibration (shaft with fluid flow, fixed–fixed).

The mode shape of modes 1–3 according to the above equation are compared with the experimental result in Figs 8–10. We find all the theoretical mode shapes are in agreement with the experimental counterparts.

Although some discrepancies due to the practical clamping and sealing are seen, the experiments conducted in this section have confirmed the general agreement between the

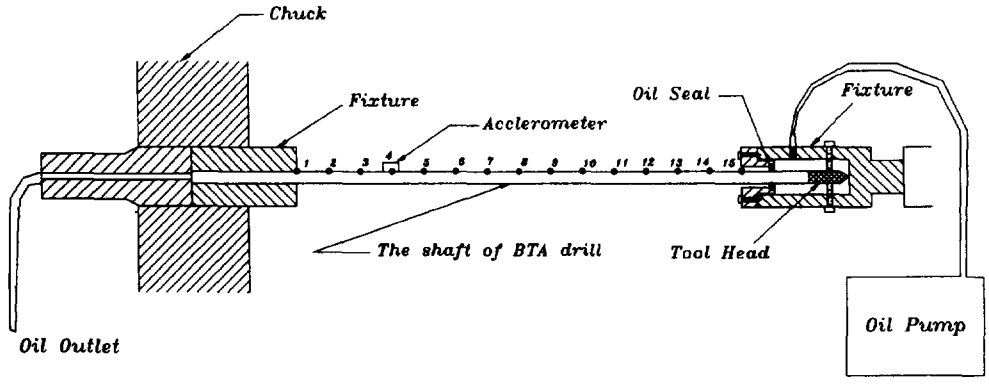

Fig. 11. The arrangements of experiment (shaft conveying fluid).

practical fixture effects and the ideal boundary conditions. This is very encouraging for future research since mathematical tools are obtained for this conventionally empirical area.

7. THE SHAFT BEHAVIOR OF THE BTA DRILL WITH CUTTING FLUID

In this section, the behavior of the shaft conveying fluid is investigated. The arrangements of this experiment are shown in Fig. 11.

The fluid pressure on the tool head P_l is read from a pressure gauge to be:

$$P_l = 3.92 \times 10^6 \text{ N/m}^2.$$

Due to the limit of the available hydraulic system the flow rate cannot be changed. We have

$$\text{Flow rate} = 1.2 \times 10^{-4} \text{ m}^3/\text{s}$$

$$\text{Flow velocity} = 1.155 \text{ m/s}.$$

The equation of motion is:

$$EI_s \frac{\partial^4 X}{\partial s^4} - \frac{\partial}{\partial s}(N - PA_f)\frac{\partial X}{\partial s} + \rho_s A_s \frac{\partial^2 X}{\partial t^2} + \rho_f A_f \left(\frac{\partial}{\partial t} - U\frac{\partial}{\partial s}\right)^2 X + C\frac{\partial X}{\partial t} = 0 \quad (43)$$

with B.C.'s

$$s = 0, \quad X = \frac{\partial X}{\partial s} = 0$$

$$s = l, \quad X = \frac{\partial X}{\partial s} = 0.$$

In this experiment, the axial force N is zero. Rearranging the above equation yields

$$EI_s \frac{\partial^4 X}{\partial s^4} + (P_l A_f + \rho_f A_f U^2)\frac{\partial^2 X}{\partial s^2} - 2\rho_f A_f U \frac{\partial^2 X}{\partial s \partial t} + (\rho_s A_s + \rho_f A_f)\frac{\partial^2 X}{\partial s^2} + C\frac{\partial X}{\partial t} = 0. \quad (44)$$

Let

$$X(s, t) = \Sigma \phi(s)\, q(t)$$

the mode shape function $\phi_j(s)$ is

$$\phi_j(s) = \cosh \beta_j s - \cos \beta_j s - \alpha_j(\sinh \beta_j s - \sin \beta_j s) \quad (45)$$

Table 4. The natural frequencies of lateral vibration of the shaft of BTA drill (both ends clamped horizontally, conveying fluid)

Mode	Theoretical values (Hz)	Experimental values (Hz)
1	43.424	43.015
2	119.689	112.382
3	234.634	220.889

and

$$\alpha_j = \frac{\cosh \beta_j l - \cos \beta_j l}{\sinh \beta_j l - \sin \beta_j l}$$

$$\cosh \beta_j l \cdot \cos \beta_j l = 1.$$

Giving an impulse to the shaft, the equation of motion becomes

$$EI_s \frac{\partial^4 X}{\partial s^4} + (P_l A_f + \rho_f A_f U^2) \frac{\partial^2 X}{\partial s^2} - 2\rho_f A_f U \frac{\partial^2 X}{\partial s \partial t} + (\rho_s A_s + \rho_f A_f) \frac{\partial^2 X}{\partial t^2} + C \frac{\partial X}{\partial t} = h(t).$$

By doing the Fourier Transform of the above equation and solving for the closed form solution, we can obtain

$$H_j(w) = \frac{1}{\left(1 - \frac{w^2}{\frac{EI_s \beta_j^4 \phi + (P_l A_f + \rho_f A_f U^2)\beta_j^2 \phi''}{(\rho_s A_s + \rho_f A_f)\phi}}\right) - i\left(\frac{w}{\frac{EI_s \beta_j^4 \phi + (P_j A_f + \rho_f A_f U^2)\beta_j^2 \phi''}{c_j \phi - 2\rho_f A_f U \beta_j \phi'}}\right)}. \tag{46}$$

The theoretical natural frequency is equal to

$$f_n = \frac{1}{2\pi} \sqrt{\frac{EI_s\ \beta_j^4 \phi + (P_l A_f + \rho_f A_f U^2)\beta_j^2 \phi''}{(\rho_s A_s + \rho_f A_f)\phi}}. \tag{47}$$

The frequency response function is

$$H(s_s, s_r, w) = \sum_{j=1}^{M} \phi_j(s_s)\ \phi_j(s_r)\ H_j(w).$$

a. Natural frequency

Comparing the theoretical values of natural frequencies of modes 1–3 with those of experiment in Table 4, we can find the theoretical values of natural frequencies being close to the experimental values.

b. Mode shape

The mode shape function of the shaft is

$$\phi_j(s) = \cosh \beta_j s - \cos \beta_j s - \frac{\cosh\ \beta_j l - \cos\ \beta_j l}{\sinh\ \beta_j l - \sin\ \beta_j l} (\sinh\ \beta_j s - \beta_j s).$$

The theoretical and experimental mode shapes are compared in Figs 12–14. It is seen that the agreements are satisfactory, but the fluid has caused even larger discrepencies.

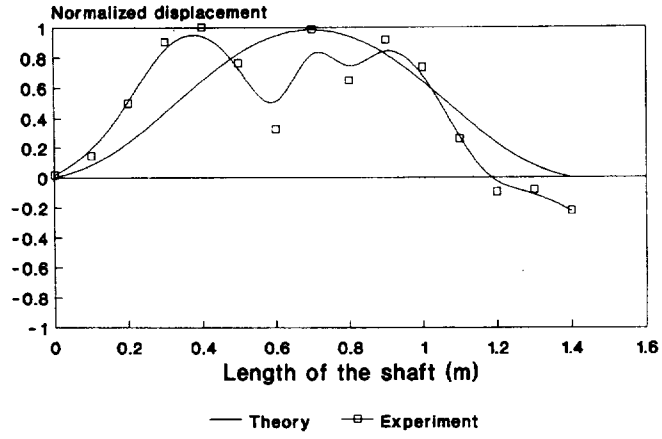

Fig. 12. The shape of mode 1 for lateral vibration (shaft with fluid flow, fixed–fixed).

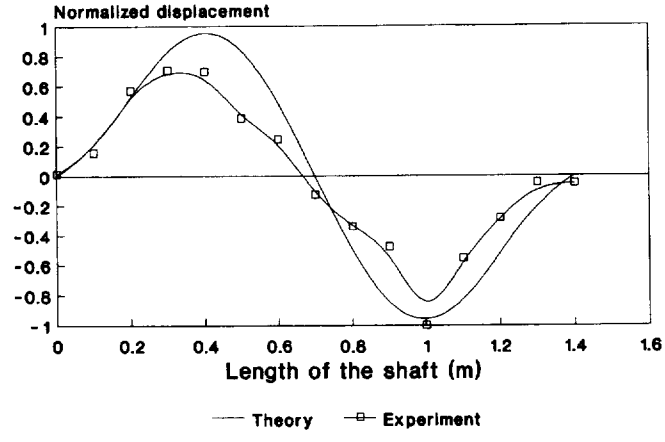

Fig. 13. The shape of mode 2 for lateral vibration (shaft with fluid flow, fixed–fixed).

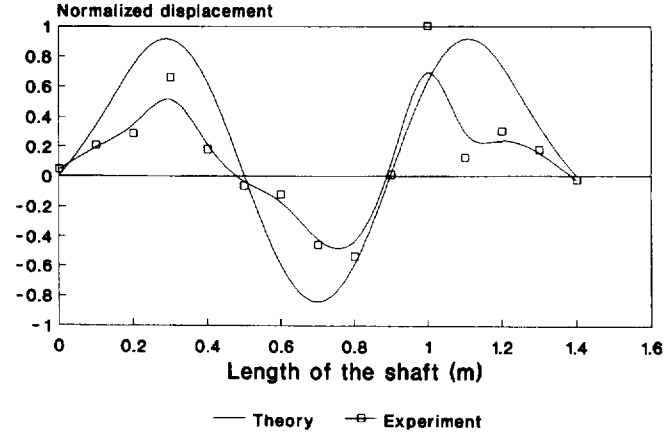

Fig. 14. The shape of mode 3 for lateral vibration (shaft with fluid flow, fixed–fixed).

8. CONCLUSION

The shaft behavior of deep hole drilling is important in the cutting process but rarely studied. This paper studied the tool shaft of deep hole drilling by treating the shaft as a pipe and using the Bernoulli–Eulerian theory. The general equations of motion for the BTA drill shaft are rigorously derived which can be reduced to different specific equations of former

works. The constructed general equations govern the lateral, longitudinal and torsional motion of a tool shaft conveying pressurized fluid.

The solutions for lateral and longitudinal motion are obtained by combined analytical and Galerkin methods.

A preliminary comparison between theoretical and experimental results shows that the rotatory inertia effect is negligible and the term $\rho I \frac{\partial^4 x}{\partial x^2 \partial t}$ in the shaft dynamics can be deleted. The shaft can be treated as an Euler Beam.

Two series of experiments are performed to verify the lateral shaft dynamics for an installed tool with and without cutting fluid. Although the boundary conditions of fixture damping are not ideal, the comparisons of natural frequencies and shaft mode shapes between theoretical and experimental results are satisfactory. Since the natural frequencies are lower than those of usual cutting tools, and the rotating workpiece might worsen these values, it can be predicted that the shaft dynamics are not negligible in the cutting process.

The constructed general equations of motion for a tool shaft build a foundation of knowledge about it and pave the way for future studies concerning correlation between cutting process and shaft behavior.

Acknowledgement—The authors thank the National Science Council of the Republic of China for the support of this study under the Grant Number NSC-81-0401-E-009-13.

REFERENCES

1. E. Flegel, Deephole drilling machine and tools for economic drilling operations. *Industrial Prod. Engng* **9**, pp. s22, s24, s26, s28 (1985).
2. P. Rudd and I. Hetherington, Advances in precision holemaking. *Manuf. Engng* **102**, 87–89 (1989).
3. P. K. R. Rao and M. S. Shunmugam, Accuracy and surface finish in BTA drilling. *Int. J. Prod. Res.* **25**, 31–44 (1987).
4. P. K. .R. Rao and M. S. Shunmugam, Investigation: stress in boring trepanning association machining. *Wear* **119**, 89–100 (1987).
5. P. K. R. Rao and M. S. Shunmugam, Analysis of axial and transverse profiles of holes obtained in B.T.A. machining. *Int. J. Machine Tools Manuf.* **27**, 505–515 (1987).
6. P. K. R. Rao and M. S. Shunmugam, Wear studies in boring trepanning association drilling. *Wear* **124**, 33–43 (1988).
7. M. M. El-Khabeery, M. M. Saleh and M. R. Ramadan, Some observations of surface integrity of deep drilling holes. *Wear* **142**, 331–349 (1991).
8. J. Corney and B. Griffiths, A study of the cutting and burnishing operation during deep hole drilling and its relationship to drill wear. *Int. J. Prod. Res.* **14**, 1–9 (1976).
9. K. Sakuma, K. Taguchi and A. Katsuki, Study on deep-hole-drilling with solid-boring tool—the burnishing action of guide pads—and their influence on hole accuracies. *Bull. JSME* **23**, 1921–1928 (1980).
10. K. Sakuma, K. Taguchi and A. Katsuki, Study on deep-hole boring by BTA system solid boring tool—behavior of tool and its effect on profile of machined hole. *Bull. Japan Soc. Precision Engng* **14**, 143–148 (1980).
11. A. Katsuki *et al.* The influence of tool geometry on axial hole deviation in deep drilling: comparison of single- and multi-edge tools. *JSME* **30**, 1167–1174 (1987).
12. M. G. Yumshtyk and S. S. Kedrov, Gun drill vibration in deep drilling. *Machines & Tooling* **39**, 34–36 (1968).
13. K. Sakuma, K. Taguchi and A. Katsuki, Self-guiding action of deep-hole-drilling tools. *Ann. CIRP* **30**, 311–315 (1981).
14. Catalog, *Drilling Tools*, HV-1200:2-ENG, SANDVIK Coromant (1983).
15. J. H. Chin, J. S. Wu and R. S. Young, The computer simulation and experimental analysis of chip monitoring for deep hole drilling. *ASME, J. Engng Indust.* **115**, 184–192 (1993).
16. J. H. Chin and J. S. Wu, Mathematical models and experiments for chip signals of single-edge deep hole drilling. *Int. J. Machine Tools Manuf.* **33**, 507–519 (1993).
17. J. H. Chin and S. A. Lin, Dynamic modelling and analysis of deep hole drilling process, *Proc. Pacific-Rim Int. Conf. Modelling, Simulation and Identification*, IASTED, Vancouver, pp. 131–134 (1992).
18. S. Chandrashekhar, T. S. Sankar and M. O. M. Osman, A stochastic characterization of the machine tool workpiece system in BTA deep hole machining—Part I. Mathematical modelling and analysis. *Adv. Manuf. Processes* **2**, 37–69 (1987).
19. S. Chandrashekhar, T. S. Sankar and M. O. M. Osman, A stochastic characterization of the machine tool workpiece system in BTA deep hole machining—Part II. Response analysis and evaluation of the tool tip motion. *Adv. Manuf. Processes*, Vol. **2**, 71–104 (1987).
20. R. D. Blevins, *Flow-Induced Vibration*, Chapter 10. Krieger Publ. (1986).
21. M. P. Paidoussis, Dynamics of Tubular cantilevers conveying fluid. *J. Mech. Engng Sci.* **12**, 85–103 (1970).
22. M. P. Paidoussis and N. T. Issid, Dynamic stability of pipes conveying fluid. *J. Sound Vibr.* **33**, 267–294 (1974).

23. M. Yoshizawa *et al.* Buckling and postbuckling behavior of a flexible pipe conveying fluid. *Bull. JSME* **28**, 1218–1225 (1985).
24. J. M. T. Thompson and T. S. Lunn, Static elastic formulations of a pipe conveying fluid. *J. Sound Vibr.* **77**, 127–132 (1981).
25. T. S. Lundgren, P. R. Sethna and A. K. Bajaj, Stability boundaries for flow induced motions of tubes with an inclined terminal nozzle. *J. Sound Vibr.* **64**, 553–571 (1979).
26. W. S. Edelstein, S. S. Chen and J. A. Jendrzejczyk, A finite element computation of the flow-induced oscillations in a cantilevered tube. *J. Sound Vibr.* **107**, 121–129 (1986).
27. J. L. Hill and C. P. Swanson, Effects of lumped masses on the stability of fluid conveying tubes. *ASME J. Appl. Mech.* 494–497. June (1970).
28. Y. Sugiyama *et al.* Effect of a spring support on the stability of pipes conveying fluid. *J. Sound Vibr.* **100**, 257–270 (1985).
29. A. E. H. Love, *A Treatise on the Mathematical Theory of Elasticity*, 4th Ed. Chapter XVIII. New York (1994).
30. J. M. Gere and S. P. Timoshenko, *Mechanics of Materials*, 2nd Ed. Wadsworth (1984).
31. D. E. Newland, *Mechanical Vibration Analysis and Computation.* John Wiley (1989).
32. R. W. Fox and A. T. McDonald, *Introduction to Fluid Mechanics*, 3rd Ed. John Wiley (1989).
33. D. J. Ewin, *Modal Testing: Theory and Practice.* Research Studies Press (1986).
34. H. Goldstein, *Classical Mechanics*, 2nd ed. The Southeast Book Co. (1989).
35. E. A. Brandes, *Metal Reference Book*, 6th Ed. Butterworths (1983).
36. W. F. Chen and T. Atsuta, *Theory of Beam-Columns*, Vol. 2. *Space Behavior and Design*, Chapter 2. McGraw-Hill (1977).
37. J. H. Chin and L. W. Lee, A study on the tool eigenproperties of BTA deep hole drill—theory and experiments. Accepted by *Int. J. Machine Tools Manuf.* (1994).
38. D. J. Gorman, *Free Vibration Analysis of Beams and Shafts.* John Wiley (1975).
39. Japanese Standards Association, *JIS 1987–1988 Ferrous Materials and Metallurgy.*
40. R. B. Ross, *Metallic Materials Specification Handbook*, 4th Ed. Chapman & Hall (1992).
41. R. H. Sabersky, A. J. Acosta and E. G. Hauptmann, *Fluid Flow a First Course in Fluid Mechanics*, 3rd Ed. Macmillan (1989).
42. W. T. Thomson, *Theory of Vibration with Applications*, 3rd Ed. Prentice-Hall (1988).
43. F. S. Tse, I. E. Morse and R. T. Hinkle, *Mechanical Vibrations Theory and Applications*, 2nd Ed. The Southeast Book Co. (1979).